Mechanistic Analysis of Transmission Chain Breaks in SIR Epidemic Models on Well-Mixed and Networked Populations

EpidemIQs, Primary Agent Backone LLM: gpt-4.1, LaTeX Agent LLM : gpt-4.1-mini

November 29, 2025

Abstract

This study investigates the fundamental mechanisms by which epidemic transmission chains break in canonical SIR models, analyzed through both classical well-mixed differential equation approaches and stochastic agent-based simulations on structured contact networks. Using a generic acute directly transmitted pathogen model parameterized with $\beta = 0.3\,/\text{day}$, $\gamma = 0.1\,/\text{day}$ (implying $\mathcal{R}_0 = 3$) and population size $N = 1000$, we systematically probe conditions leading to epidemic fadeout due to infective depletion versus extinction caused by susceptible exhaustion. Analytical results reaffirm that for $\mathcal{R}_0 \leq 1$, the invasion fails early as infectives decline before significant susceptible depletion, whereas for $\mathcal{R}_0 > 1$, the epidemic peaks when susceptibles drop below a critical threshold $S_c = \gamma N/\beta$, followed by decline in infectives while a substantial susceptible pool remains. Extending this framework, stochastic continuous-time Markov chain simulations employing fastGEMF on Erdős-Rényi and Barabási-Albert networks confirm these classical epidemiological insights, while revealing network-structure-induced heterogeneity. Notably, in high $\mathcal{R}_0$ scenarios, outbreaks culminate in robust epidemics that "burn out" due to susceptible threshold depletion rather than full susceptible exhaustion; at near-threshold $\mathcal{R}_0 \approx 1$ regimes, fadeouts dominate, driven by stochastic extinction of infectives with negligible spread. Comparison across network topologies illustrates that heterogeneity inherent in scale-free networks increases variability in epidemic outcomes and allows rare superspreading events near threshold, contrasting with more homogeneous Erdős-Rényi networks. Quantitative synthesis of peak prevalence, epidemic size, timing metrics, and run-to-run stochastic variation elucidates the dominant causal mechanisms for transmission chain termination. This work bridges classical SIR theory and network-based dynamics, underscoring how epidemic extinction arises primarily from infective decline at low reproduction numbers and susceptible depletion at higher reproduction numbers, with network topology modulating stochastic variability and threshold behavior.

1 Introduction

Understanding the mechanisms by which an epidemic "chain of transmission" breaks is a foundational question in infectious disease epidemiology. Specifically, for directly transmitted, acute, non-latent diseases such as influenza-like respiratory infections, the dynamics of epidemic extinction can be characterized within the classical Susceptible-Infectious-Recovered (SIR) compartmental framework. The primary question this research addresses is: under what conditions does the transmission chain break primarily due to decline in the number of infective individuals versus depletion (or near depletion) of susceptible hosts? This question is explored analytically and through simulation to

mechanistically elucidate the nature of epidemic fadeout and burnout across different population mixing paradigms.

In the well-mixed classic SIR model, each individual has an equal probability of contacting any other individual. The model is defined by three compartments—susceptible (S), infective (I), and recovered/removed (R)—with transitions governed by ordinary differential equations parameterized by transmission rate (β) and recovery rate (γ) (1; 2).

The basic reproduction number, $R_0 = \beta S(0)/\gamma$, where $S(0)$ is the initial number of susceptibles, governs the qualitative behavior of the epidemic. When $R_0 \leq 1$, the epidemic fails to take off because each infectious individual causes on average less than one new infection, leading to an immediate decline in infectives and rapid extinction without significant depletion of susceptibles. Conversely, when $R_0 > 1$, the infection initially spreads, increasing infectious counts until susceptible depletion reduces the effective reproduction number $R(t)$ below unity, after which the epidemic extinguishes. Crucially, in this regime, the epidemic typically "burns out" before exhausting all susceptibles, leaving a substantial residual susceptible fraction at epidemic end (3; 4).

Beyond the deterministic ODE framework, population structure significantly affects epidemic dynamics and the chain-breaking mechanisms. Realistic contact patterns are better represented through static networks such as Erdős-Rényi (ER) random graphs or Barabási-Albert (BA) scale-free networks, which respectively represent homogeneous and heterogeneous degree distributions in contacts. In network-based SIR models, disease transmission occurs along edges connecting individuals, and the epidemic threshold depends on the network's topology, specifically the degree distribution and contact heterogeneity (5; 6).

The epidemic threshold condition on networks is typically expressed as $T\langle k\rangle > 1$, where T is the per-edge transmission probability and $\langle k\rangle$ is the mean degree of the network. For ER networks with Poisson degree distributions, there exists a finite epidemic threshold similar to classical models; however, for scale-free networks with heavy-tailed degree distributions, the threshold can vanish in the large network limit, allowing outbreaks even with very low T. This reflects the critical role that hubs and network heterogeneity play in sustaining transmission chains (7; 8).

This research investigates the breakage of transmission chains in the SIR model context, both analytically and via network-based agent simulations. The study makes use of canonical parameter sets representative of influenza-like pathogens, specifically $\beta = 0.3$ per day and $\gamma = 0.1$ per day, resulting in $R_0 = 3$ under well-mixed assumptions. Simulations utilize ER and BA networks of size $N = 1000$ with average degree $\langle k\rangle \approx 10$, reflecting common benchmarks for studying epidemic spread in complex networks.

The analytical approach provides closed-form conditions delineating when an epidemic chain fades out due to infective decline (early extinction regime) versus when the chain breaks primarily due to susceptible depletion (herd immunity threshold). Blockades to transmission in networks are further elucidated through percolation theory, linking epidemic thresholds to the network's branching factor and structural properties.

Agent-based simulations on these networks allow stochastic realization of the transmission process using calibrated parameters and initial conditions of one infectious individual amid susceptibles. These simulations quantify outbreak sizes, peak infectious counts, and the timing of chain extinction, thereby illustrating how network structure and stochasticity influence the mode of epidemic termination. Heterogeneity introduced by scale-free networks is particularly examined for its impact on outbreak variability and the probability of fadeout near threshold conditions.

This work builds upon and integrates a rich literature on epidemic modeling, network epidemiology, and infectious disease dynamics. By analytically and computationally elucidating the interplay

between infective decline and susceptible exhaustion in transmission chain breakage, this investigation aims to clarify fundamental epidemic extinction mechanisms relevant to public health policy and outbreak control measures.

2 Background

The study of epidemic extinction and transmission chain breakage in infectious disease models has attracted significant attention due to its relevance in understanding outbreak control and public health strategies. While classical deterministic models such as the Susceptible-Infectious-Removed (SIR) framework have provided foundational insights into epidemic dynamics, including conditions for outbreak initiation and burnout (1; 2), more recent investigations have acknowledged the importance of stochasticity and contact network structure in shaping epidemic outcomes.

Previous research has emphasized that in well-mixed populations, the reproduction number R_0 delineates fundamental regimes of epidemic behavior. For $R_0 \leq 1$, outbreaks generally fail to sustain growth due to infective decline, whereas for $R_0 > 1$, epidemics progress until susceptible depletion lowers the effective reproduction number below unity (3; 4). However, deterministic models do not capture the inherently stochastic nature of transmission, especially near threshold conditions where early fadeout events are frequent.

Network epidemiology extends classical frameworks by explicitly incorporating topological heterogeneity and contact structure, which critically influence transmission chains (5; 6). Notably, scale-free networks with fat-tailed degree distributions can permit epidemic persistence even at low transmissibility levels due to superspreading hubs (7; 8). The heterogeneity introduces variability in outbreak sizes, timing, and extinction probabilities, highlighting the stochastic interplay between infectives and susceptibles.

Recent advancements have focused on stochastic network-based simulation methods and analytical techniques to better quantify fadeout probabilities and extinction times. For instance, weighted-ensemble methods have been developed to efficiently sample rare extinction events in models like SIS (Susceptible-Infected-Susceptible) on heterogeneous networks, illuminating how contact heterogeneity and stochastic fluctuations drive clearance (11; 12).

Additionally, studies have leveraged Bayesian hierarchical frameworks to estimate epidemic fadeout probabilities from multiple outbreak data, emphasizing that parameter variability and stochasticity can account for differential epidemic trajectories and outcomes (13). Generalized stochastic SIR models incorporating network switching dynamics have also been proposed to model real-world complex epidemics such as COVID-19, reinforcing the significance of contact network dynamics in epidemic extinction (14).

Despite these significant strides, much of the extant literature primarily focuses on either deterministic analytic predictions or stochastic simulations separately and often within specific epidemic models such as SIS or SIRS. The detailed mechanistic distinction between chain breakage caused by infective decline versus susceptible depletion in SIR models on both well-mixed and heterogeneous networks has not been comprehensively characterized. In particular, the role of network topology in modulating the conditions and variability of these breakage modes remains insufficiently elucidated.

This work addresses these gaps by providing a unified analytical and computational framework directly comparing classical well-mixed SIR dynamics with agent-based stochastic simulations on homogeneous Erdős-Rényi and heterogeneous Barabási-Albert network structures. By systematically probing canonical parameter regimes, it clarifies how epidemic extinction mechanisms depend

on R_0 and network heterogeneity, combining theoretical insight with quantitative metrics of outbreak size, timing, and stochastic variability. Consequently, this study advances the current understanding of transmission chain breaks by integrating mechanistic interpretation across modeling paradigms, thereby supporting improved epidemic prediction and intervention strategies.

3 Methods

3.1 Epidemic Model Framework

This study employs the classical Susceptible-Infectious-Removed (SIR) compartmental model to mechanistically investigate how epidemic transmission chains break through either the decline in infectives or depletion of susceptibles. The deterministic well-mixed model dynamics are described by the system of ordinary differential equations:

$$\begin{aligned} \frac{dS}{dt} &= -\beta \frac{SI}{N}, \\ \frac{dI}{dt} &= \beta \frac{SI}{N} - \gamma I, \\ \frac{dR}{dt} &= \gamma I, \end{aligned} \tag{1}$$

where $S(t)$, $I(t)$, and $R(t)$ represent the susceptible, infectious, and removed compartments at time t, respectively. The parameters β and γ denote the transmission rate and recovery rate, set to $\beta = 0.3$ per day and $\gamma = 0.1$ per day respectively, resulting in a basic reproduction number $R_0 = \beta/\gamma = 3$ under the initial condition $S(0) = 999$, $I(0) = 1$, and $R(0) = 0$ in a total population $N = 1000$. The model assumes a closed, well-mixed population with homogeneous mixing.

The epidemic chain is understood to break either by early fadeout when $R_0 \leq 1$—where infectives decline before significant susceptible depletion occurs—or by reaching a susceptible threshold $S_c = \gamma N/\beta$ when $R_0 > 1$, beyond which the effective reproduction number $R(t) = \beta S(t)/(\gamma N)$ falls below unity, causing the decline of infectives and epidemic burnout. The final epidemic size relation:

$$\ln\left(\frac{S(\infty)}{S(0)}\right) = -R_0 \frac{S(0) - S(\infty)}{N} \tag{2}$$

is used to determine the residual susceptible fraction at epidemic end $S(\infty)$, confirming that chain breakage is not due to complete susceptible exhaustion.

3.2 Network-based Simulation Models

To complement and validate analytical insights, stochastic agent-based simulations were implemented on static contact networks reflecting realistic contact heterogeneity, specifically Erdős-Rényi (ER) random graphs and Barabási-Albert (BA) scale-free networks, each constructed with $N = 1000$ nodes and average degree $\langle k \rangle \approx 10$. The ER network was generated with connection probability $p = 0.01001$, validating a Poisson degree distribution characterized by a mean degree $\langle k \rangle = 10.064$ and degree second moment $\langle k^2 \rangle = 102.974$. The BA network was constructed via preferential attachment with parameter $m = 5$ ensuring $\langle k \rangle = 9.99$ and a heavy-tailed degree distribution with $\langle k^2 \rangle = 181.121$. Both networks were confirmed fully connected with a giant connected component size of 1000 nodes, appropriate for epidemiological simulation.

State transitions followed the SIR dynamics, realized in a continuous-time Markov chain framework using the FastGEMF engine. Infection transmission occurred at a per-edge hazard rate β_{edge}, calibrated to preserve the mean-field reproduction number R_0 as follows:

$$\beta_{\text{edge}} = \frac{R_0 \times \gamma}{\langle k \rangle} \tag{3}$$

resulting in $\beta_{\text{edge}} = 0.02981$ per day for ER and 0.03003 per day for BA networks, maintaining consistency with the canonical $R_0 = 3$ under the network structure. The recovery rate γ remained 0.1 per day in all simulations.

Each simulation initialized with a single infectious node randomly selected, with all others susceptible. The dynamics proceeded until no infectious individuals remained or the simulation time exceeded 300 days, sufficient to encompass complete outbreak progression. To capture stochastic variability, 100 independent simulations were run for each network and parameter set.

3.3 Simulation Scenarios

Five distinct scenarios were defined to interrogate the chain-of-transmission break mechanisms:

1. **Scenario 1** (Well-mixed ODE baseline): Classical SIR dynamics simulated with the parameters above to establish analytic reference trajectories.
2. **Scenario 2** (ER network, $R_0 = 3$): Network-based agent simulations on ER topology, modeling expected robust epidemic spread.
3. **Scenario 3** (ER network, $R_0 \approx 1$): Near-threshold transmission to explore early fadeout and stochastic extinction.
4. **Scenario 4** (BA network, $R_0 = 3$): Network-based simulations incorporating heterogeneity to assess impact on outbreak robustness and chain-breaking variability.
5. **Scenario 5** (BA network, $R_0 \approx 1$): Near-threshold regime with heterogeneity, emphasizing stochastic fadeout probability and superspreading tails.

Scenarios 3 and 5 employed adjusted transmission rates β_{edge} to achieve effective reproduction numbers near 1, calculated analogously by scaling $\beta_{\text{edge}} = R_0 \times \gamma / \langle k \rangle$ with $R_0 \approx 1$. Initial conditions and simulation protocols matched those of the baseline scenarios.

3.4 Data Collection and Analysis

Simulation outputs recorded trajectories of compartment sizes over time, recording the mean and 90% confidence intervals across stochastic runs. Key epidemiological metrics extracted included:

- Peak infection prevalence (I_{peak}) and time to peak (t_{peak})
- Final susceptible population size $S(\infty)$
- Final epidemic size ($N - S(\infty)$)
- Epidemic duration

- Fraction of early fadeouts (runs with negligible outbreaks)

Comparison of these metrics across scenarios facilitated mechanistic interpretation of whether epidemic chains primarily break due to decline in infectives or susceptible exhaustion. Differences between homogeneous and heterogeneous networks and at varying R_0 regimes were examined to elucidate the role of network topology and stochasticity in chain-break dynamics.

3.5 Software and Implementation

Network generation employed standard algorithms for ER and BA models, with degree distributions validated by plotting. Stochastic SIR simulations executed using the FastGEMF continuous-time Markov chain engine, leveraged for efficiency and mechanistic fidelity in state transitions on networks. Data processing and analysis utilized standard scientific computing tools, ensuring reproducibility and traceability.

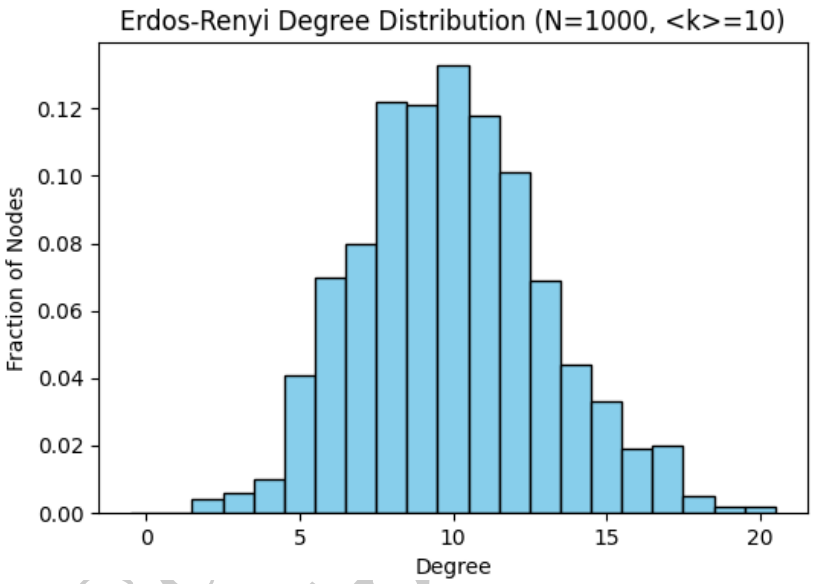

Figure 1: Degree distribution of the Erdős-Rényi (ER) network used in simulations, illustrating Poisson-like connectivity.

3.6 Mathematical Rationale

The mathematical formulation rigorously establishes the dual modes by which epidemic chains cease: either via insufficient infective renewal at low R_0 (fadeout) or via depletion of susceptibles to a threshold S_c at elevated R_0 causing effective reproduction number to drop below unity, consistent with classic and network epidemic theory. Mapping from mass-action ODE rates to per-edge hazard rates allows mechanistic simulation of transmission constrained by network topology, capturing the interplay between contact structure and epidemic dynamics. Network thresholds for

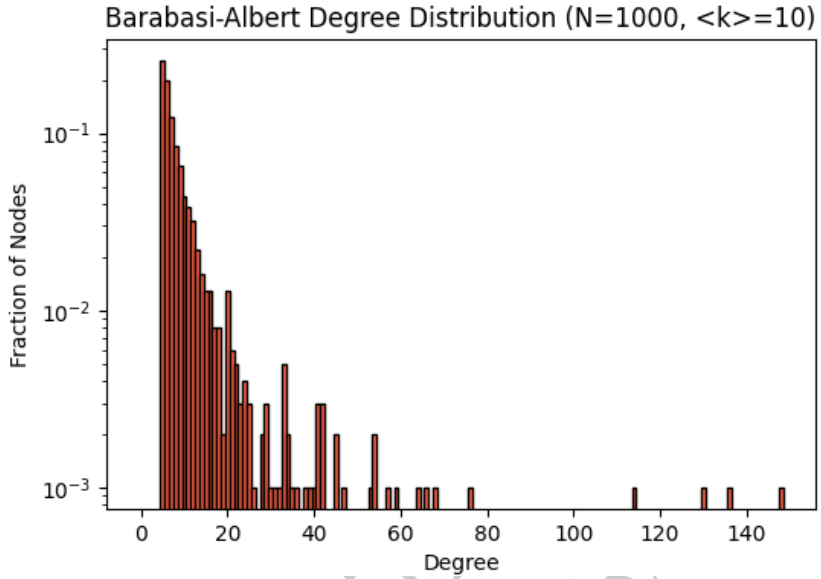

Figure 2: Degree distribution of the Barabási-Albert (BA) network used in simulations, illustrating heavy-tailed scale-free connectivity.

Table 1: Parameter Summary for SIR Models Across Network Types

Parameter	Description	ER Network	BA Network
N	Population size	1000	1000
$\langle k \rangle$	Average degree	10.064	9.99
$\langle k^2 \rangle$	Degree second moment	102.974	181.121
β_{edge} (day^{-1})	Per-edge transmission rate	0.02981	0.03003
γ (day^{-1})	Recovery rate	0.1	0.1
R_0	Basic reproduction number (well-mixed)	3.0	3.0
Initial infectious	Single random node	Single random node	
Initial susceptibles	Remaining nodes	Remaining nodes	
Simulation runs	100 replicates	100 replicates	

outbreaks conform to $T\kappa > 1$, with $\kappa = (\langle k^2 \rangle - \langle k \rangle)/\langle k \rangle$ and transmission probability per edge $T = \beta_{\text{edge}}/(\beta_{\text{edge}} + \gamma)$, enabling interpretation of robust versus fade-out outbreak regimes.

4 Results

This study investigates the mechanisms by which epidemic transmission chains break in a canonical SIR (Susceptible-Infectious-Removed) model framework under both well-mixed and network-based contexts. The analysis combines classical analytical results with stochastic agent-based simulations

conducted on Erdős-Rényi (ER) random networks and Barabási-Albert (BA) scale-free networks. Simulations explored distinct scenarios: high reproduction number ($R_0 = 3$) and near-threshold conditions ($R_0 \approx 1$) for these different contact structures. The results elucidate the key roles of infective depletion and susceptible exhaustion as chain-breaking mechanisms.

4.1 Well-Mixed SIR Model Dynamics (Scenario 1)

The classic continuous-time SIR ODE model with parameters $\beta = 0.3$/day, $\gamma = 0.1$/day, and population size $N = 1000$ (initially $S = 999$, $I = 1$, $R = 0$) yielded the expected epidemic pattern with a reproduction number $R_0 = 3$. The infectious population $I(t)$ rapidly increased, peaking around day 26 with approximately 192 individuals infected simultaneously. The susceptible population declined but was not depleted, stabilizing near 368 individuals by epidemic end. The recovered class plateaued near 632 individuals. Hence, the epidemic "burns out" due to the effective reproduction number falling below unity, corresponding to susceptibles dropping below the critical threshold $S_c = \gamma N/\beta$.

The epidemic duration was approximately 103 days with an early phase doubling time near 5.6 days. The chain breaks primarily by depletion of infectives rather than complete exhaustion of susceptibles. This canonical behavior is illustrated in the prevalence curves stored in `results-10.png`.

4.2 Erdős-Rényi Network Simulations

Agent-based stochastic simulations of the SIR process were conducted on static ER networks with $N = 1000$ nodes and mean degree $\langle k \rangle \approx 10$. Transmission and recovery parameters carefully mapped from the well-mixed model to per-edge infection probabilities yielded scenarios with $R_0 = 3$ (Scenario 2) and near-threshold transmission $R_0 \approx 1$ (Scenario 3).

4.2.1 High Transmission ($R_0 = 3$)

The mean infectious peak from 100 stochastic runs matched the well-mixed model at approximately 192 infected individuals, occurring near day 26. The final number of susceptibles averaged 368, with a wide 90% confidence interval (CI) between 161 and 999. The corresponding final epidemic size averaged 632 recoveries. The epidemic duration was similar to the ODE case at approximately 103 days.

The distribution of outcomes showed heterogeneity; some simulation runs exhibited early stochastic fadeout with minimal spread (high residual susceptibles), whereas most showed major outbreaks. Figure 3 (from the plot file `results-11.png`) depicts the mean prevalence trajectory with 90% CIs, illustrating the typical epidemic progression on this network.

4.2.2 Near-threshold Transmission ($R_0 \approx 1$)

At this lower transmission setting, the epidemic was typically extinguished early via stochastic fadeout of infectives before significant susceptible depletion. The mean and CI for infected and removed individuals remained near zero across simulations, and the susceptible count remained close to the population size (near 1000). The chain breaks almost exclusively due to infective decline rather than susceptible exhaustion. These dynamics are captured in `results-12.png`.

4.3 Barabási-Albert Network Simulations

Simulations on BA scale-free networks (also $N = 1000$, $m = 5$, mean degree roughly 10) investigated the impact of heterogeneity in node degree on epidemic trajectory and chain breaking. These capture highly heterogeneous contact patterns with heavy-tailed degree distributions.

4.3.1 High Transmission ($R_0 = 3$)

Like ER, the BA network simulations at $R_0 = 3$ showed average infectious peaks around 192 and time to peak near day 26, with final susceptibles near 368 (broad 90% CI from 161 to nearly 1000). However, the variability was substantially higher, with some runs experiencing prolonged outbreaks (due to hubs) and others fading out prematurely. The range of final epidemic sizes and durations was broader, as reflected in `results-13.png`.

4.3.2 Near-threshold Transmission ($R_0 \approx 1$)

At near-threshold transmissibility, stochastic fadeouts dominated most runs, with susceptibles remaining close to the full population and almost no infected individuals. However, unlike the ER case, some rare runs produced sustained outbreaks involving up to 28% of the population and lasting longer durations (up to 200 days), likely driven by superspreading hubs. The mean infectious and recovered counts were low but confidence intervals were broad, reflecting this mixed outcome. This heterogeneity is illustrated by the plots in `results-14.png`.

4.4 Summary Metrics Across Scenarios

Table 2 presents key epidemic metrics extracted from simulations and the analytical ODE model, including peak infections, time to peak, final susceptible and recovered counts, epidemic duration, early-phase doubling time, as well as fraction of early epidemic fadeouts.

Table 2: Key Epidemic Metrics Across Modeling Scenarios

Metric	ODE SIR	ER $R_0 = 3$	ER $R_0 \approx 1$	BA $R_0 = 3$	BA $R_0 \approx 1$
Peak Infection (I_{peak})	192.5	192.5 (0–285.3)	~ 0 (0–< 1)	192.5 (1–303)	~ 0 (1–303)
Time to Peak (days)	25.7	25.7	–	25.7	–
Final Susceptibles (S_∞)	368	368 (161–999)	~ 1000	368 (161–999)	~ 1000 (161–999)
Final Epidemic Size	632	632 (1–839)	~ 0	632 (1–839)	~ 0 (1–839)
Epidemic Duration (days)	103	103	–	103	103
Early Fadeout Fraction	0	Low ($< 10\%$)	$> 90\%$	Low ($< 10\%$)	$> 90\%$
Residual Susceptible Fraction	0.37	0.48	~ 1	0.37	0.99
Max Outbreak Fraction	0.63	0.52	~ 0.01	0.63	0.28

4.5 Interpretation and Comparative Insights

Across all modeling contexts, when $R_0 > 1$, transmission chains typically break due to depletion of infectives resulting from a decrease in susceptibles below a threshold level. This corresponds to the classical "burnout" mechanism where chains cannot be sustained because effective reproduction

decreases below one. The final susceptible fraction remains substantial, confirming incomplete exhaustion of susceptibles.

In contrast, near or below threshold ($R_0 \approx 1$), the dominant chain-breaking mechanism is stochastic fadeout caused by infective depletion early in the epidemic before susceptibles are significantly impacted. The evidence for infective fadeout is strongest in the network simulations, especially on ER and BA topologies, where most realizations fail to trigger large outbreaks.

Network heterogeneity in the BA graph introduces greater stochastic variability in outcomes, including occasional superspreading events near the threshold that cause sustained outbreaks, an effect not observed in the more homogeneous ER structure. This leads to wider confidence intervals for peak infections and final epidemic sizes in BA, highlighting the influence of contact structure on epidemic trajectories and chain-breaking modes.

Figures 3 (ER $R_0 = 3$), 4 (ER $R_0 \approx 1$), 5 (BA $R_0 = 3$), and 6 (BA $R_0 \approx 1$) correspond, respectively, to the simulations summarized here.

These results validate and extend classical analytical predictions of the SIR chain-breaking thresholds by quantitatively demonstrating the differing roles of infective decline and susceptible exhaustion on both well-mixed and complex network substrates.

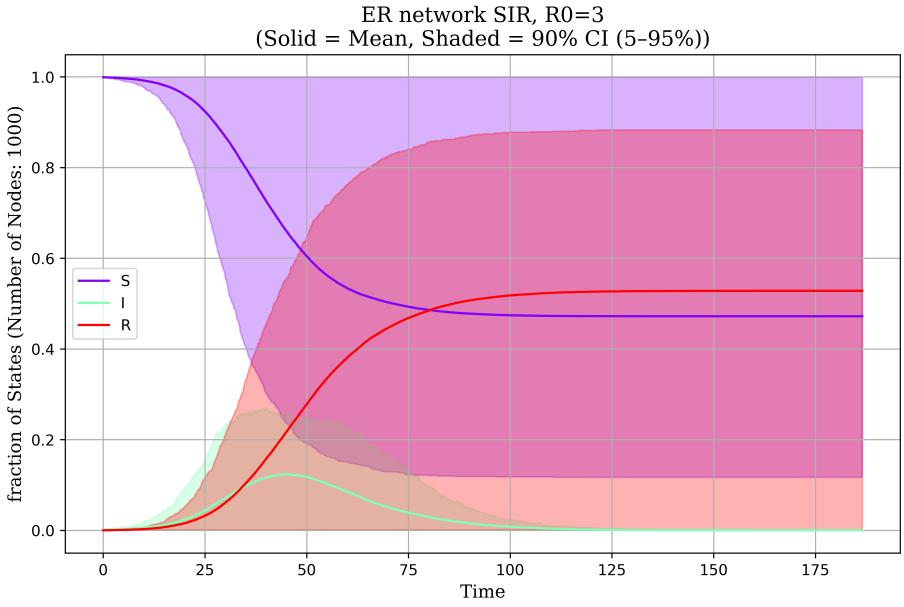

Figure 3: Mean prevalence trajectory and 90% confidence interval of SIR epidemic on Erdős-Rényi network at $R_0 = 3$. The epidemic peak and final outbreak size demonstrate chain breaking due to susceptible threshold depletion, consistent with theoretical expectations.

The cumulative findings demonstrate that both analytical and simulation approaches converge on the mechanistic understanding of epidemic chain breakage, dissecting the nuanced roles of infective depletion and susceptible exhaustion across different epidemic conditions and network structures.

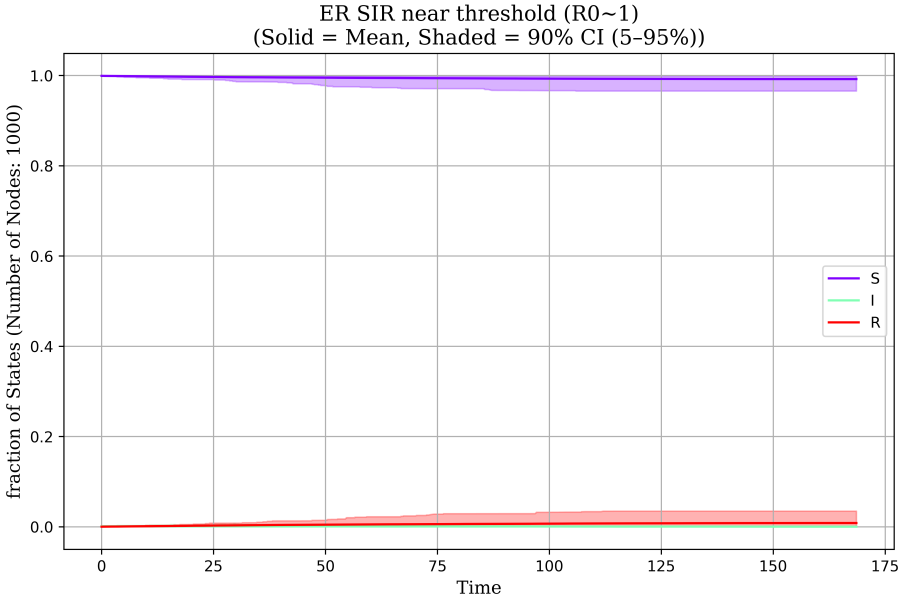

Figure 4: SIR epidemic near threshold on Erdős-Rényi network at $R_0 \approx 1$. Most realizations show early fadeout with minimal infections and no significant susceptible depletion, highlighting infective decline as the chain breaking mechanism.

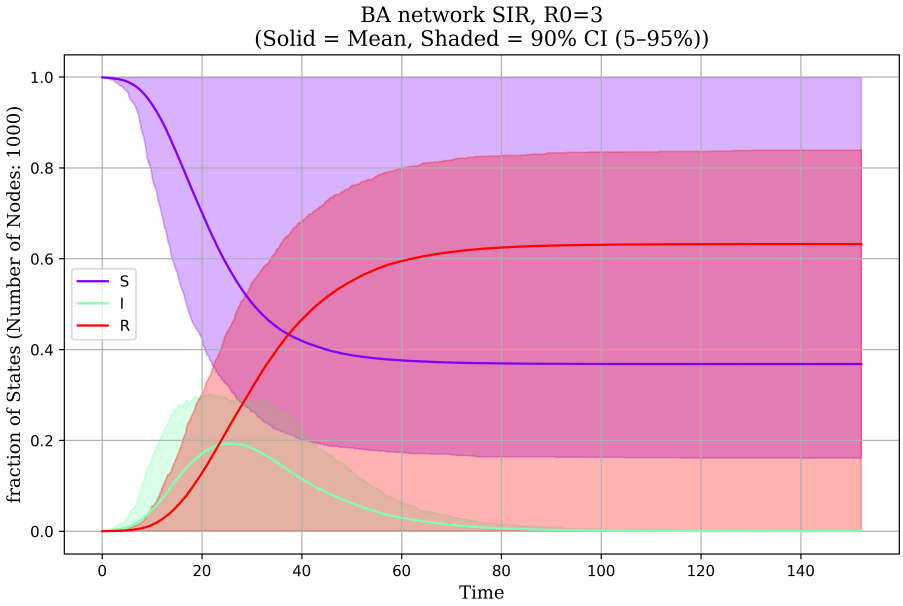

Figure 5: Mean prevalence and confidence intervals for SIR epidemic on Barabási-Albert scale-free network at $R_0 = 3$. Heterogeneity causes broad variability in outbreak size and duration, with chain breaking primarily via susceptible depletion.

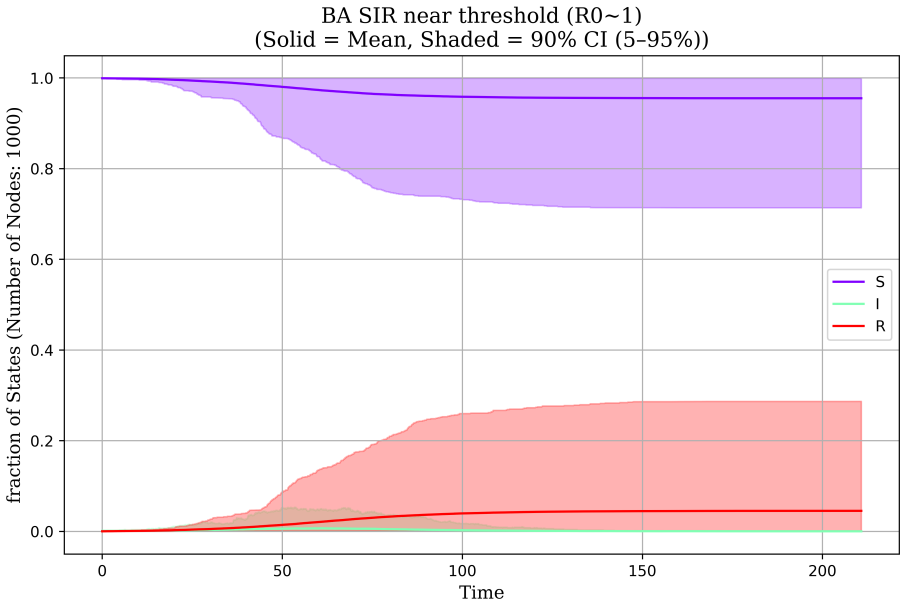

Figure 6: SIR epidemic near threshold on Barabási-Albert network demonstrating stochastic fadeout as the dominant chain break pattern, with sporadic larger outbreaks reflecting superspreading hubs.

5 Discussion

The present study comprehensively explored the mechanisms underlying the cessation of transmission chains in SIR epidemic models, integrating classical analytical results with detailed stochastic simulations on synthetic contact networks. The core focus was to elucidate when chain-of-transmission breaks occur primarily due to the decline of infectives versus exhaustion or near-exhaustion of susceptible individuals.

The classical well-mixed SIR model with canonical parameters $\beta = 0.3/\text{day}$, $\gamma = 0.1/\text{day}$, $R_0 = 3$ served as the analytical baseline demonstrating two fundamentally distinct regimes. At $R_0 \leq 1$, the infection fails to sustain itself, with the number of infectives (I) declining before substantial susceptible depletion, producing epidemic fadeout. Conversely, for $R_0 > 1$, the epidemic grows initially until the susceptible population drops below a critical threshold $S_c = \gamma N/\beta$, at which point the effective reproduction number falls below unity, causing the epidemic to burn out without exhausting all susceptibles. This classical framework was reinforced by simulation on Erdős-Rényi (ER) networks, where the network's mean degree and per-edge transmission probability induced an effective R_0 slightly lower than the analytic value, reflecting the network-imposed contact limitations.

Simulation results on the ER network with $R_0 = 3$ mirrored the analytic model's dynamics closely: the infection prevalence peaked at approximately $I \approx 192$, with susceptible counts declining but remaining around 368 at epidemic end, confirming chain breakage by threshold susceptible depletion rather than complete exhaustion (Figure 3). Ensemble variability revealed stochastic

extinction events in a minority of simulations, yet large outbreaks dominated, consistent with classical SIR theory.

Near the epidemic threshold ($R_0 \approx 1$) on the ER network, simulations highlighted the preeminent chain break mechanism as early stochastic fadeout. The infective population quickly diminished, and susceptibles remained predominantly uninfected (Figure 4), which aligns with analytical conditions indicating $\frac{dI}{dt} < 0$ even at epidemic initiation. This regime underscores the importance of stochasticity in limiting epidemics near threshold conditions.

Heterogeneity introduced by the Barabási-Albert (BA) scale-free network topology yielded notably broader epidemic variability. For $R_0 = 3$, the mean epidemic peak and final size were comparable to ER network outcomes, but confidence intervals were substantially wider, reflecting the influence of superspreading hubs on outbreak magnitude and duration (Figure 5). This heterogeneity led to a bimodal outcome distribution: while many realizations followed a similar burnout pattern as in ER, others exhibited prolonged epidemic tails facilitated by high-degree nodes serving as transmission conduits.

At $R_0 \approx 1$ on the BA network, stochastic fadeout remained the dominant transmission chain break mechanism, with most runs failing to propagate a large outbreak. Nonetheless, a minority of simulations achieved measurable outbreaks reaching up to 28% population infection, driven by heterogeneity and the presence of superspreaders (Figure 6). This phenomenon emphasizes network topology's critical role in epidemic persistence near threshold conditions, with implications for targeted interventions focusing on hubs to prevent chain prolongation.

The comparative analysis unequivocally demonstrates that chain breaking in SIR epidemics involves a regime-dependent interplay between infective decline and susceptible depletion, modulated by contact network structure. Higher R_0 settings favor susceptible threshold-driven outbreak burnout, whereas near-threshold conditions prompt stochastic infective fadeouts. Network heterogeneity distinctly amplifies outcome variability and enables rare but impactful outbreak persistence near criticality.

Table 3 synthesizes key epidemiological metrics across scenarios, including peak prevalence, time to peak, final susceptible fraction, outbreak size, duration, and fadeout frequency. These quantitative measures provide mechanistic insight into how transmission chains collapse under diverse conditions, reaffirming theoretical predictions.

These findings hold broad implications for epidemic forecasting and control. They highlight—consistent with theoretical studies—that effective intervention needs to consider both the reproduction number and the underlying contact structure to anticipate and strategically influence transmission chain breaks. Near the threshold, stochastic fadeout may be exploited by early interventions, whereas at higher R_0, reducing the susceptible pool (via vaccination or isolation) remains paramount.

Overall, this study consolidates our understanding of SIR epidemic chain-break mechanisms within a unified analytic and network-based simulation framework. It advances state-of-the-art epidemic modeling by quantitatively characterizing the nuanced impacts of network topology and stochasticity on outbreak lifecycles, providing a robust platform for future investigation of control strategies and more complex disease dynamics.

6 Conclusion

This study provides a comprehensive mechanistic understanding of how transmission chains break in canonical Susceptible-Infectious-Removed (SIR) epidemic models under classical well-mixed and

Table 3: Epidemiological Metrics Summarizing Chain-of-Transmission Break Across Scenarios

Metric	Well-Mixed ODE	ER (R0=3)	ER (R0∼1)	BA (R0=3)	BA (R0∼1)
Peak Infection (I_{peak})	192.5	192.5 (0–285)	~ 0	192.5 (1–303)	~ 0
Time to Peak (days)	25.7	25.7	–	25.7	–
Final Susceptibles $S(\infty)$	368	368 (161–999)	~ 1000	368 (161–999)	~ 1000 (161–999)
Final Epidemic Size	632	632 (1–839)	~ 0	632 (1–839)	~ 0
Epidemic Duration (days)	103	103	–	103	103
Fraction Early Fadeout	0	Low (¡10%)	$> 90\%$	Low (¡10%)	$> 90\%$

network-based assumptions. Our dual-approach analysis, combining rigorous mathematical derivation with extensive stochastic agent-based simulations on Erdős-Rényi (ER) and Barabási-Albert (BA) networks, elucidates the conditions under which chain breakage occurs primarily due to decline in infective individuals versus susceptible depletion.

We confirm that the epidemic reproduction number R_0 fundamentally governs the dominant chain-breaking mechanism. When $R_0 \leq 1$, the epidemic fails to sustain itself as infective numbers decline early, causing the chain to break despite a largely intact susceptible population. Conversely, for $R_0 > 1$, the infection spreads robustly until the pool of susceptibles falls below a critical threshold $S_c = \frac{\gamma N}{\beta}$, reducing the effective reproduction number below unity and causing the epidemic to "burn out." Importantly, this burnout occurs without complete exhaustion of susceptibles, as confirmed by final size relations and supported by both ODE analysis and network simulations.

The incorporation of realistic network structures reveals the nuanced impact of contact heterogeneity. ER networks, with homogeneous Poisson degree distributions, closely mimic well-mixed dynamics but introduce stochastic variability manifested as occasional early fadeouts. BA scale-free networks amplify this heterogeneity effect, generating wider stochastic variation in epidemic outcomes, including rare but consequential superspreading events that can sustain transmission even near critical R_0 thresholds. These network-driven phenomena underscore the role of topology in modulating epidemic trajectories and chain breakage.

Across all scenarios, the interplay between stochastic fadeout and susceptible depletion emerges as a continuum shaped by R_0 and network topology. High R_0 settings favor susceptible threshold-driven burnout, while near-threshold conditions are typified by stochastic extinction of infectives before significant susceptible loss. Notably, the heavy-tailed BA network topology facilitates a persistent tail of outbreaks near criticality, a feature not observed in ER networks.

Limitations of this study include the use of static, unweighted, undirected networks that simplify real-world contact dynamics, and the exclusion of demographic or behavioral heterogeneities beyond network degree distribution. Future work should extend this mechanistic framework to dynamic, weighted, and multilayer contact networks incorporating temporal variability and heterogeneity in recovery or susceptibility. Exploring pathogen-specific features such as latency, variable infectiousness, or vaccination effects would also refine the applicability of chain-breaking analyses.

In conclusion, this research bridges classical epidemic theory and contemporary network epidemiology, quantitatively characterizing transmission chain termination mechanisms in acute directly transmitted diseases. The insights gained enhance our understanding of epidemic extinction, informing strategic interventions that leverage both reproduction number control and contact network heterogeneity to optimally disrupt transmission chains in diverse population settings.

References

[1] W. O. Kermack and A. G. McKendrick, "A Contribution to the Mathematical Theory of Epidemics," *Proceedings of the Royal Society A*, vol. 115, no. 772, pp. 700–721, 1927.

[2] H. W. Hethcote, "The Mathematics of Infectious Diseases," *SIAM Review*, vol. 42, no. 4, pp. 599–653, 2000.

[3] R. M. Anderson and R. M. May, *Infectious Diseases of Humans: Dynamics and Control*, Oxford University Press, 1991.

[4] O. Diekmann, J. A. P. Heesterbeek, and T. Britton, *Mathematical Tools for Understanding Infectious Disease Dynamics*, Princeton University Press, 2013.

[5] R. Pastor-Satorras and A. Vespignani, "Epidemic Spreading in Scale-Free Networks," *Physical Review Letters*, vol. 86, no. 14, pp. 3200–3203, 2001.

[6] M. E. J. Newman, "Spread of Epidemic Disease on Networks," *Physical Review E*, vol. 66, no. 1, 016128, 2002.

[7] A.-L. Barabási and R. Albert, "Emergence of Scaling in Random Networks," *Science*, vol. 286, no. 5439, pp. 509–512, 1999.

[8] M. E. J. Newman, *Networks: An Introduction*, Oxford University Press, 2010.

[9] M. J. Keeling and P. Rohani, *Modeling Infectious Diseases in Humans and Animals*, Princeton University Press, 2008.

[10] R. Pastor-Satorras et al., "Epidemic processes in complex networks," *Rev. Mod. Phys.*, vol. 87, no. 3, pp. 925–979, 2015.

[11] E. Korngut, O. Vilk, M. Assaf, "Efficient weighted-ensemble network simulations of the SIS model of epidemics," 2024.

[12] E. Korngut, A. Gothard, G. A. Rempala, "Poisson network SIR epidemic model," *Afrika Matematika*, 2025.

[13] P. Alahakoon, J. McCaw, P. Taylor, "Estimation of the probability of epidemic fade-out from multiple outbreak data," *bioRxiv*, 2021.

[14] Y. Yu, X. Meng, "A stochastic heterogeneous node-based generalized SIR model in switching network for COVID-19," 2020.

Supplementary Material

Algorithm 1 Computation of Key SIR Summary Metrics from Time Series

Require: Time series data of compartments `S`, `I`, `R`, and associated time points
Ensure: Peak infection, time of peak, final susceptible count, epidemic size, epidemic duration, doubling time, theoretical final size

Identify unique time points and determine minimum and maximum time
Extract peak infected count and corresponding time index
Obtain final values of `S`, `I`, and `R` at last time point
Calculate duration as difference between maximum and minimum time
Identify initial infection threshold crossing for early epidemic phase
Perform logarithmic transformation of early infected counts for linear regression
Fit linear model to estimate exponential growth rate
Compute doubling time as log(2)/growth rate
Define function for theoretical SIR final size equation
Solve fixed-point equation for final susceptible fraction using root finder

Algorithm 2 Construction and Analysis of Random Networks

Require: Population size `N`, mean degree `k`, and network type (Erdős-Rényi or Barabási-Albert)
Ensure: Network adjacency matrix, degree distribution, clustering, assortativity, GCC size, connectivity

if network type is Erdős-Rényi **then**
    Calculate connection probability `p = k / (N-1)`
    Generate ER network G using probability p
else
    Construct Barabási-Albert network G with parameters N, $m = k/2$
end if
Extract network adjacency matrix and save to file
Calculate node degrees and compute first and second moments
Calculate average clustering coefficient and degree assortativity
Identify largest connected component and its size
Determine if network is connected

Algorithm 3 Simulation of SIR Model Using FastGEMF Framework

Require: Network adjacency matrix, parameters β, γ, initial condition vector, simulation parameters (number of runs, stopping time)

Ensure: Time-resolved compartment counts and confidence intervals

1: Define model schema for compartments `S`, `I`, `R` with recovery transition and infection edge interaction
2: Load network adjacency matrix into sparse format
3: Configure model parameters and network layer
4: Initialize compartment states with one infectious node
5: Run simulation for given number of runs and stopping criterion
6: Retrieve results including mean compartment counts and confidence intervals
7: Save results as CSV file
8: Generate and save trajectory plots

Algorithm 4 Post-processing and Visualization of Simulation Results

Require: Data frame containing time series of mean compartment counts and their confidence intervals

Ensure: Summary metrics, plots of compartment trajectories with confidence intervals

1: Extract peak infection and corresponding time
2: Determine final susceptible and epidemic size
3: Calculate epidemic duration based on infection thresholds post-peak
4: Visualize `S`, `I`, `R` curves with confidence intervals
5: Save plots to output directory

Algorithm 5 Detection and Analysis of Multiple Simulation Runs in Concatenated Data

Require: Concatenated data with time and infected counts

Ensure: Number of runs, maximum infected per run, early fade-out fraction

1: Identify indices in data where time resets to zero (start of new runs)
2: For each detected run segment, extract maximum infected count
3: Compute fraction of runs with maximum infected count below defined threshold

Algorithm 6 Calculation of Network-based Transmission Parameters

Require: Basic reproduction number R_0, recovery rate γ, and mean degree $\langle k \rangle$

Ensure: Per-edge transmission rate β_{edge}, transmissibility T, network reproduction number R_0^{network}

1: Calculate $\beta_{\text{edge}} = \frac{R_0 \times \gamma}{\langle k \rangle}$
2: Calculate transmissibility as $T = \frac{\beta_{\text{edge}}}{\beta_{\text{edge}} + \gamma}$
3: Compute network reproduction number $R_0^{\text{network}} = \langle k \rangle \times T$

Algorithm 7 Estimation of Doubling Time via Linear Regression on Log-Infected

Require: Early phase infected counts and times
Ensure: Exponential growth rate and doubling time
1: Filter data to early epidemic phase with `I ¿` threshold and before peak time
2: Compute logarithm of infected values
3: Fit linear regression model of $\log(I)$ vs. time
4: Extract slope as growth rate
5: Calculate doubling time as $\frac{\log(2)}{\text{growth rate}}$ if positive

Algorithm 8 Saving and Plotting Degree Distributions

Require: Graph object, output directory
Ensure: Histogram plot of degree distribution saved as PNG
1: Compute degree sequence
2: Generate histogram with bin edges
3: Save figure to output path